International Journal of
Electrical and Computer System Design
ISSN: 2582-8134 www.ijecsd.com

Radiation Detection on Abandoned Uranium Mines on the Navajo Nation

Roshonda Shurly[1], Dr Sundaram Arumugam[2], Dr. Peter Romine[3]

roshonda.shurley@student.navajotech.edu, sarumugam@navajotech.edu, promine@navajotech.edu

[1,3] Electrical Engineering Navajo Technical University, USA

Abstract: From 1944 to 1986, the United States government extracted uranium ore from the Navajo Nation reservation. The Navajo Nation is a part of northeastern Arizona, southeastern Utah, and northwestern New Mexico totaling 17,545,000 acres of land. The Navajo Nation is a beautiful and sacred homeland to over 250,000 people. Today, the Navajo Nation is scattered with over 500 abandoned uranium mines. The radiation from the uranium mine is a national health and environmental hazard to the Navajo community. Unmanned aerial vehicles (UAVs), or drones, are great candidates for radiation monitoring and environmental testing contamination. For this project, we will select a radiation detector to mount onto a UAV to test the radiation levels of abandoned uranium mines. Thorough research will be conducted on what radiation detector will be used and why we chose this detector. We will also use the programming language Python to create an algorithm that will capture the radiation levels from a data set that was received from the United States Geological Survey. The United States Geological Survey collected data from a magnetometer field and the data set will be imported into python.

Keywords: Unmanned aerial vehicles; Uranium; Radiation

1. Introduction

Uranium mining plays a significant role in global energy production. However, the extraction and processing of uranium ore pose potential health and environmental hazards due to radiation exposure. In particular, uranium mines are known to emit radiation that can have detrimental effects on human health and ecosystems [1]. This article aims to shed light on the radiation risks associated with uranium mines, the safety measures employed to mitigate these risks, and the importance of monitoring and regulating radiation levels in the mining industry [2].

Uranium is a natural radioactive element that emits alpha and beta particles with a small amount of gamma radiation. It is applied in nuclear power plants, nuclear reactors, and weapons. It has three forms of isotopes, U-234, U-235, and U-238. Radiation categories fall into four aspects: alpha, beta, gamma/x-ray particles, and neutrons. Gamma rays have a high-energy photon that can release the nucleus during decay. They are release from the decay of all radioactive isotopes including alpha and beta emission which make them a good candidate for detectors. There is a variety of gamma ray detectors such as plastic scintillators, sodium iodide scintillators, germanium detectors, lanthanum bromide detectors, and cadmium zinc telluride detectors.

Proceeding of "Technology Integration for Sustainable Development: An International E-Conference on Electrical, Electronics, Computer Science and Mechanical Engineering. (EECM-2023)". Organized by SJUIT.

2. Literature Review

Evaluation of Unmanned Aerial Vehicles for Radiation Detection proposed in [3] go into depth with their research and specify the different types of radiation and radiation detectors that are out there. The article specifies that there are four types of radiation which are alpha, beta, gamma ray/x-ray, and neutrons. Alpha radiation is a charged particle with two protons and two neutrons [4]. Alpha particles are a common decay that comes from an isotope of a high atomic number. Examples of radioactive elements are thorium, uranium, and plutonium. They can travel from 1 to 2 inches in the air and can be shielded by a piece of paper.

Beta radiation is an electron that is emitted from decay of radioactive isotopes. The beta particles can travel faster than alpha particles which they are able to have longer range. They are small particles that can travel to 10 feet in the air and can be shielded by aluminum, plastic, and skin [5].

Gamma rays are released from decay from all radioactive isotopes even from alpha and beta emissions. Gamma rays and x-ray have a neutral charged particle that can travel more than 100 feet. It is shielded by high hydrogen content material. Neutrons have electromagnetic waves or photons [7]. They have no mass or charged particles

which can travel several hundreds of feet in the air and can penetrate through the body. It is shielded by dense materials such as lead, concrete, and steel

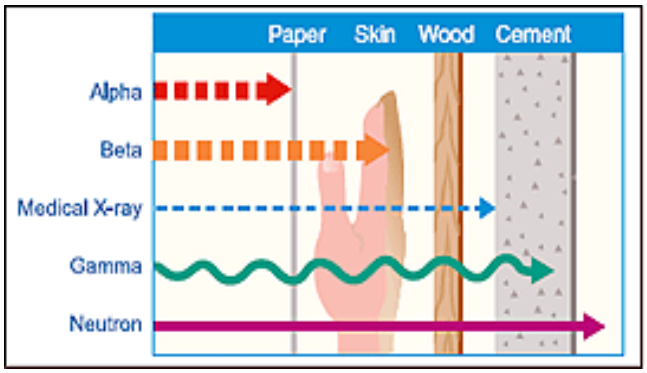

Fig.1. Radioactive isotopes

Gamma ray detectors are primarily an efficient detector especially when it comes to radiation detection applications using UAVs. The five common types of gamma ray detectors are plastic scintillators, sodium iodide scintillators, high purity germanium detectors, lanthanum bromide detectors, and cadmium zinc telluride detectors. Each gamma ray detector plays a vital role and has its own characteristics.

In summary, a plastic scintillator is a low-cost detector that can be made large, it is robust, and does not require much maintenance. One of the disadvantages of using this detector is its lack of resolution and it does not have the capability of identifying the radiation source. High purity germanium detectors have one of the best resolutions for detecting gamma spectroscopy. The disadvantages of using a high purity germanium detector is that they require to be cryogenically cooled down and are expensive. Lanthanum bromide detectors can operate at room temperature and have a slightly better energy resolution. The disadvantage of using this detector is that they don't have large crystals which prevent to go long range [8].

Cadmium zinc telluride detectors is a semiconductor that can convert x-ray or gamma photons into electrons and holes. They have a higher energy resolution, detect low energetic particles, operate at room temperature, have high atomic number and density. Sodium iodide scintillators detectors have high luminescence efficiency and are available in a variety of sizes. They also operate at room temperature and the crystals can be large but are more expensive than plastic scintillators [9].

For UAV application, we believe that the best detectors for this project will be the sodium iodide scintillators and the cadmium zinc telluride detectors.

RADIATION DETECTOR: CADMIUM ZINC TELLURIDE

A semiconductor detector is a radiation detector that ionize radiation. The semiconductor detector is a solid-state that is made from silicon or germanium. Its main purpose is to measure and detect the effects of nuclear particles such as alpha particles, gamma radiation, and photons [10].

Semiconductors operate differently from insulators and metals. It is because of its intermediate band gap also known as an energy gap. Energy gap is described as the energy difference between the electrons in the valence and conduction band.

The electrons in the valence band are bound to the atom which prevents them from moving around freely but the electrons in the conduction band are free to move around. When the electrons move from the valence band to the conduction band they are able to conduct electricity. Metals and conductors are the ones that can produce electricity. The valence band and conduction band in semiconductors are so close to one another that they can conduct electricity. The valence band and conduction band in metals overlap or are close to one another so that they can produce electricity as well. These are many reasons why semiconductors are great candidates for detectors [11].

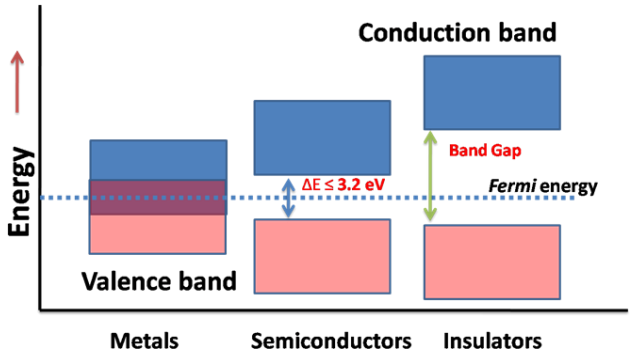

Fig.2. Semiconductor detector

The article, "Development of Airborne Gamma-Ray Spectrometer Based on a CZT detector" by Young-Yong Ji, Sungyeop Joung, Byung Il Min, and Kyung-Suk Suh. They mention the importance of how environmental radiation measurement has increased rapidly in the pass years and the significance to having a proper response to a radiation exposure. To prevent any human contact from entering a radiation exposure, they built an unmanned aerial vehicle (UAV) integrated with an airborne gamma-ray spectrometry. This UAV was used at Japan Atomic Energy Agency (JAEA). The airborne gamma-ray spectrometer was made of three parts and

that was signal processing unit, Global Positioning System (GPS), Bluetooth interface, and battery pack. The dose rate maps were made from aerial surveys at the flight height of 1 m above the ground. The radiation system was called MARK-A1 (Monitoring of Ambient Radiation of KAERI-Airborne) which consists of CZT (cadmium zinc telluride) detector, signal processing unit, positioning and interface unit. The CZT detector was the size of 10x10x5 mm weighing about 1 kg. The measurement from the ambient dose rate, the dose conversion was added to the measured energy spectrum during the flight. For the calculation, a dose conversion from the CZT detector was made from Monte Carlo stimulation. The aerial measurements were conducted at 10 m height and 1 ms speed. The maximum flight time was 10 minutes. The data was configured through Bluetooth interface from ground.

The article, “Characterization of CZT Detectors for the ASIM Mission,” by Carl Budtz-Jørgensen, Irfan Kuvvetli, Member, IEEE, Yngve Skogseide, Kjetil Ullaland, and Nikolai Ostgaard summarizes the selection and characterization of the CZT detector crystals in x and gamma rays instruments. The National Space Institute of Technical University of Denmark focused on the expected spectra performance of the detector and found the unexplained pixel to pixel count rate variations.

3. Methodology

A CSV data set was received from the United States Geological Survey. The data will depict the radiation levels that were captured from a magnetometer field. The CSV file was imported into a python script. The algorithm or script will be used on future data sets when they are captured from the abandoned uranium mine. Below is a screenshot of the script that was taken from Jupyter notebook, and it will show the steps that were taken to create this algorithm using python coding (Fig.3). Below is also a description of what each row of code does and their purpose.

Steps of python code and description of each code:

1st step:

#import the command/library functions into the script
1. import numpy as np
Importing numpy helps with high level mathematical functions such as arrays and matrices. More importantly it will help with computing the longitude, latitude, and values for the magnetic field.
2. import geopandas as gpd
Importing geopandas is an ideal support that helps improve geographic data to pandas objects. The components and usage of working with geospatial data is easily operated in python. It also combines the capabilities of pandas and shapely together.

```
In [1]: import numpy as np
        import geopandas as gpd
        import matplotlib.pyplot as plt
        from pykrige.ok import OrdinaryKriging

In [2]: #Reads CSV data by using Geopandas
        data_magnetic_field = gpd.read_file('_magarrow_tethers_normal2.csv')
        #Reduce the data points
        data_magnetic_field = data_magnetic_field[::100]
        data_magnetic_field
```

Out[2]:

	Longitude	Latitude	Altitude_m	Total_Field_nT	geometry
0	584317.271	4093978.681	179.32	47529.8382	None
100	584317.802	4093979.03	179.28	47530.67315	None
200	584318.332	4093979.379	179.24	47531.04535	None
300	584318.863	4093979.728	179.2	47531.83685	None
400	584319.393	4093980.077	179.16	47532.6664	None
...	...	...	...	...	...
590800	584462.825	4094035.848	175.43	47614.93415	None
590900	584462.569	4094036.534	175.42	47616.91975	None
591000	584462.313	4094037.219	175.42	47618.6832	None
591100	584462.057	4094037.904	175.41	47619.981	None
591200	584461.801	4094038.59	175.41	47621.875	None

5913 rows × 5 columns

```
In [3]: print(data_magnetic_field.crs)

In [4]: #Latitude and longitude values
        lat_1 = np.array(data_magnetic_field['Latitude'].values, dtype='float')
        lon_1 = np.array(data_magnetic_field['Longitude'].values, dtype='float')
        val_1 = np.array(data_magnetic_field['Total_Field_nT'].values, dtype='float')

In [5]: #Define coordinates for gridded data
        ygrid = np.linspace(np.min(lat_1), np.max(lat_1), 100)
        xgrid = np.linspace(np.min(lon_1), np.max(lon_1), 100)

In [6]: #Define ordinary Kriging to get latitude, longitude, and values
        OK = OrdinaryKriging(lat_1, lon_1, val_1, variogram_model= 'linear')

In [7]: zgrid, ss = OK.execute('grid', ygrid, xgrid)

In [26]: #Plot the data
         plt.figure(figsize=(10, 5))
         plt.subplot(1, 2, 1)
         plt.scatter(lat_1, lon_1, c=val_1, cmap = "viridis")
         plt.title("USGS Point Data")

         plt.subplot(1, 2, 2)
         plt.imshow(np.flipud(zgrid), interpolation="none", cmap = "viridis")
         plt.title("USGS Gridded Data")
         plt.colorbar()
```

Fig.3. Proposed algorithm using python coding

3. import matplotlib.pyplot as plt

Importing matplotlib.pyplot helps with the command function of matplotlib and can operate like MATLAB. It can help with the functions such as creating a figure, creating a plotting area in a figure, plotting lines in a plotting area, decorating the plot with labels, etc.

4.from pykrige.ok import OrdinaryKriging

Importing pykrige.ok gives access to 2D Ordinary Kriging. 2D Ordinary Kriging is used is used to support regional-linear, point logarithmic, and external drift terms

2nd step

#Reads CSV data by using Geopandas

5. data_magnetic_field = gpd.read_file('_magarrow_tethers_normal2.csv')

geopandas is being used to read the csv file

#Reduce the data points

1. data_magnetic_field = data_magnetic_field[::100]
   - reduces the data points and only selecting every point by a 100
2. data_magnetic_field
3. print(data_magnetic_field.crs)
   - gets the current crs and prints the data return

3rd step

#Latitude and longitude values

4. lat_1 = np.array(data_magnetic_field['Latitude'].values, dtype='float')
5. lon_1 = np.array(data_magnetic_field['Longitude'].values, dtype='float')
6. val_1 = np.array(data_magnetic_field ['Total_Field_nT'].values, dtype='float')
   - helps get the values for latitude, longitude, and the values

4th step

7. ygrid = np.linspace(np.min(lat_1), np.max(lat_1), 100)
8. xgrid = np.linspace(np.min(lon_1), np.max(lon_1), 100)
   - defines the coordinates for the gridded data

5th step

9. OK = OrdinaryKriging(lat_1, lon_1, val_1, variogram_model= 'linear')
   - It defines the ordinary Kriging to get the latitude, longitude and the values

6th step

10. zgrid, ss = OK.execute('grid', ygrid, xgrid)
    - This code interpolates the values for the grid

7th step

11. plt.figure(figsize=(10, 5))
12. plt.subplot(1, 2, 1)
13. plt.scatter(lat_1, lon_1, c=val_1, cmap = "viridis")
14. plt.title("USGS Point Data")
15. plt.subplot(1, 2, 2)
16. plt.imshow(np.flipud(zgrid), interpolation="none", cmap = "viridis")
17. plt.title("USGS Gridded Data")
18. plt.colorbar()

- The code above plots the data and you can edit the plot by giving it a title, shade of color, size, etc..

Python steps without description

```
1. import numpy as np
2. import geopandas as gpd
3. import matplotlib.pyplot as plt
4. from pykrige.ok import OrdinaryKriging
5. data_magnetic_field = gpd.read_file('_magarrow_tethers_normal2.csv')
6. data_magnetic_field = data_magnetic_field[::100]
7. data_magnetic_field
8. print(data_magnetic_field.crs)
9. lat_1 = np.array(data_magnetic_field['Latitude'].values, dtype='float')
10. lon_1 = np.array(data_magnetic_field['Longitude'].values, dtype='float')
11. val_1 = np.array(data_magnetic_field['Total_Field_nT'].values, dtype='float')
12. ygrid = np.linspace(np.min(lat_1), np.max(lat_1), 100)
13. xgrid = np.linspace(np.min(lon_1), np.max(lon_1), 100)
14. OK = OrdinaryKriging(lat_1, lon_1, val_1, variogram_model= 'linear')
15. zgrid, ss = OK.execute('grid', ygrid, xgrid)
16. plt.figure(figsize=(10, 5))
17. plt.subplot(1, 2, 1)
18. plt.scatter(lat_1, lon_1, c=val_1, cmap = "viridis")
19. plt.title("USGS Point Data")
20. plt.subplot(1, 2, 2)
21. plt.imshow(np.flipud(zgrid), interpolation="none", cmap = "viridis")
22. plt.title("USGS Gridded Data")
23. plt.colorbar()
```

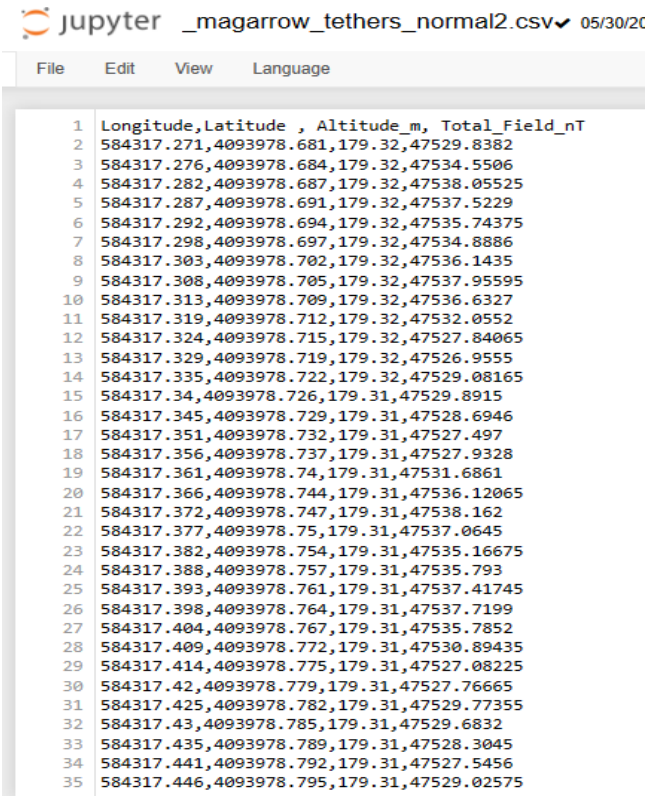
jupyter _magarrow_tethers_normal2.csv 05/30/20

File Edit View Language

```
Longitude,Latitude , Altitude_m, Total_Field_nT
584317.271,4093978.681,179.32,47529.8382
584317.276,4093978.684,179.32,47534.5506
584317.282,4093978.687,179.32,47538.05525
584317.287,4093978.691,179.32,47537.5229
584317.292,4093978.694,179.32,47535.74375
584317.298,4093978.697,179.32,47534.8886
584317.303,4093978.702,179.32,47536.1435
584317.308,4093978.705,179.32,47537.95595
584317.313,4093978.709,179.32,47536.6327
584317.319,4093978.712,179.32,47532.0552
584317.324,4093978.715,179.32,47527.84065
584317.329,4093978.719,179.32,47526.9555
584317.335,4093978.722,179.32,47529.08165
584317.34,4093978.726,179.31,47529.8915
584317.345,4093978.729,179.31,47528.6946
584317.351,4093978.732,179.31,47527.497
584317.356,4093978.737,179.31,47527.9328
584317.361,4093978.74,179.31,47531.6861
584317.366,4093978.744,179.31,47536.12065
584317.372,4093978.747,179.31,47538.162
584317.377,4093978.75,179.31,47537.0645
584317.382,4093978.754,179.31,47535.16675
584317.388,4093978.757,179.31,47535.793
584317.393,4093978.761,179.31,47537.41745
584317.398,4093978.764,179.31,47537.7199
584317.404,4093978.767,179.31,47535.7852
584317.409,4093978.772,179.31,47530.89435
584317.414,4093978.775,179.31,47527.08225
584317.42,4093978.779,179.31,47527.76665
584317.425,4093978.782,179.31,47529.77355
584317.43,4093978.785,179.31,47529.6832
584317.435,4093978.789,179.31,47528.3045
584317.441,4093978.792,179.31,47527.5456
584317.446,4093978.795,179.31,47529.02575
```

Fig.4. Steps of python code

4. Experimental Results

In the context of radiation detection on abandoned uranium mines, conducting magnetometer surveys provides valuable insights into the distribution of radioactive materials and potential environmental hazards. Accurate mapping of the flight path taken during magnetometer surveys over these sites is crucial for effective data analysis and interpretation. This article focuses on the process of generating a 2D map that represents the flight path conducted during radiation detection flights over abandoned uranium mines using magnetometer technology.

Radiation detection flights over abandoned uranium mines involve the use of magnetometers to measure magnetic variations caused by radioactive materials. Mapping the flight path is essential to ensure comprehensive coverage of the mine sites and facilitate the correlation between detected radiation levels and specific locations within the survey area. Accurate flight path mapping enhances the understanding of radiation distribution and assists in assessing potential risks to the environment and human health.

The process of creating a 2D map of the flight path for radiation detection starts by recording the aircraft's position and altitude at regular intervals using GPS and other navigation systems. These data points are then processed to generate a visual representation of the flight path taken over the abandoned uranium mines. Advanced software tools and geographic information systems (GIS) are commonly utilized to accomplish this mapping task.

Specialized mapping software, often integrated with radiation detection and data analysis tools, is employed to integrate the recorded flight data with other geospatial information. This includes topographic maps, aerial imagery, and georeferenced data related to the abandoned uranium mines. By combining these data sources, a comprehensive 2D map is created, overlaying the flight path with radiation detection readings and relevant site information.

Accurate mapping of the flight path is crucial for radiation detection on abandoned uranium mines. It allows for the identification of potential data gaps or overlapping areas, ensuring thorough coverage of the survey sites. Accurate flight path mapping also facilitates the correlation of radiation readings with specific locations, enabling a comprehensive assessment of radiation distribution within the mine sites. Additionally, it assists in quality control and validation of the collected data, ensuring reliable and robust analysis of radiation levels.

The Fig.5 below is the output from the python script. The picture shows a 2D mapping of the flight that was taken at the magnetometer field. The yellow highlight shows that the part of the region which has the highest radiation levels.

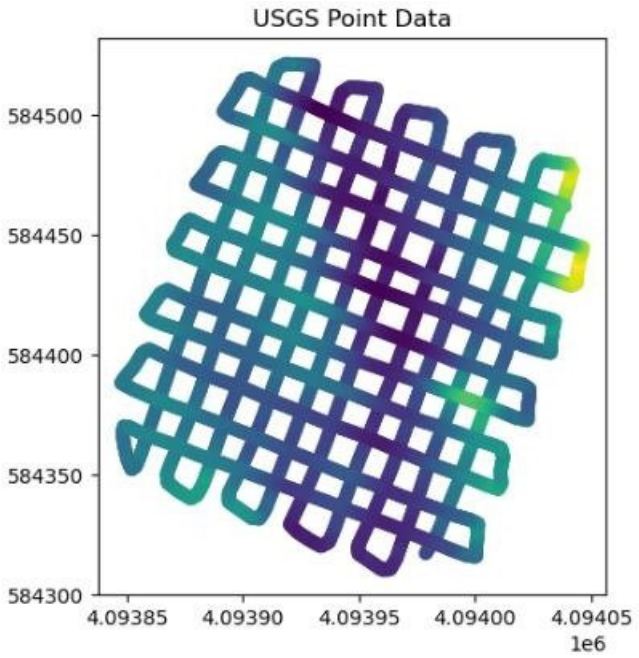

(a)

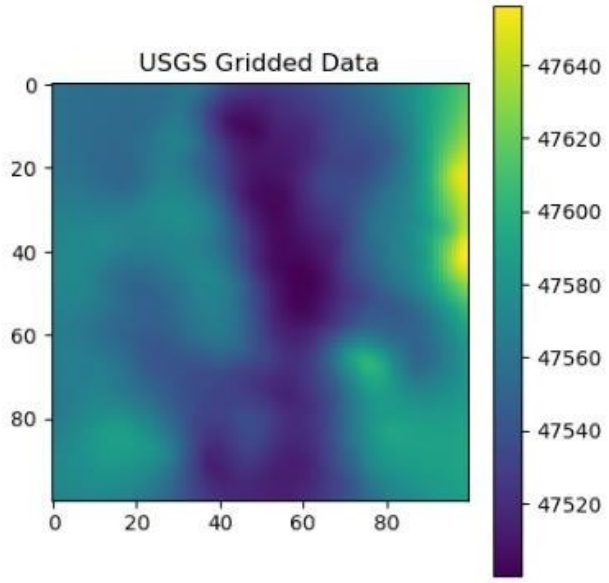

(b)

Fig.5. 2D mapping of the flight that was taken at the magnetometer field

5. Conclusion

With the proliferation of abandoned uranium mines across the Navajo Nation, the need for effective radiation monitoring and assessment is paramount. Unmanned aerial vehicles (UAVs) present a promising solution, offering the ability to collect data from inaccessible or hazardous areas. By equipping these UAVs with carefully selected radiation detectors and employing Python-based algorithms for data analysis, we can establish a comprehensive system for monitoring radiation levels in the abandoned mines. Through this project, we hope to mitigate the health and environmental risks faced by the Navajo community, fostering a safer and more sustainable future for all.

During a flight, a radiation detector needs to have good efficiency in detection, and it needs to be able to recognize its source. Overall, the radiation detector that would make a good candidate for this project is the sodium iodide and the cadmium zinc telluride detectors. This project is a long-term project that will have his events of goals to accomplish. The interns have accomplished milestones such as purchasing the drone and creating a python script that will be used once we receive data from the flight plan from the abandoned uranium mines. Below is a timeline of what next steps and actions will be taken in the next months.

- Create GIS dataset for visualization
- Buy a manufacture radiation detector
- Create flight plan for drone flights of the abandoned uranium mine
- Conduct drone flights over abandon uranium mine and capture imagery using Earth platform
- Import dataset received from the drone flight into python

Acknowledgement:

Effort Sponsored by the Government under Cooperative Agreement Number W911SR-14-2-0001, Project Award Number 65 titled “Integrative Research in Emerging Technologies for DHS Use Cases” and led by the Universities Space Research Association (USRA). The U.S. Government is authorized to reproduce and distribute reprints for Governmental purposes notwithstanding any copyright notation thereon. The views and conclusions contained herein are those of the authors and should not be interpreted as necessarily representing the official policies or endorsements, either expressed or implied, of the U.S. Government.

References:

1. E. Talnishnikh, L. Paganini, J. Stegenga, H. Limburg and H. Wörtche, "Self- sustained operation of radiation detectors based on embedded signal processing," 2013 3rd International Conference on Advancements in Nuclear Instrumentation, Measurement Methods and their Applications (ANIMMA), Marseille, France, 2013, pp. 1-6, doi: 10.1109/ANIMMA.2013.6728020.
2. Sakoda, S. Murakami, Y. Ishimori and S. Horai, "Concentration ratios of 238U and 226Ra for insects and amphibians living in the vicinity of the closed uranium mine at Ningyo-toge, Japan," in Journal of Radiation Research, vol. 61, no. 1, pp. 207-213, Dec. 2019, doi: 10.1093/jrr/rrz096.
3. Hernández-Cole, J.; Ortiz-Malavassi, E.; Moya, R.; Murillo, O. Evaluation of Unmanned Aerial Vehicles (UAV) as a Tool to Predict Biomass and Carbon of Tectona grandis in Silvopastoral Systems (SPS) in Costa Rica. Drones 2021, 5, 47. https://doi.org/10.3390/drones5020047
4. T. Marchais et al., "Characterization of Uranium Ore Samples by HPGe Gamma-Ray Spectroscopy," in IEEE Transactions on Nuclear Science, vol. 67, no. 4, pp. 654-661, April 2020, doi: 10.1109/TNS.2020.2966824.

5. T. Marchais et al., "Detailed MCNP Simulations of Gamma-Ray Spectroscopy Measurements With Calibration Blocks for Uranium Mining Applications," in IEEE Transactions on Nuclear Science, vol. 65, no. 9, pp. 2533-2538, Sept. 2018, doi: 10.1109/TNS.2018.2797312.
6. A. Geofrey, R. S. Sinde and S. F. Kaijage, "The Real-time IoT-based Monitoring Radiation Level, the Case of Mkuju River Uranium Mining," 2021 IEEE International Conference on Smart Internet of Things (SmartIoT), Jeju, Korea, Republic of, 2021, pp. 262-266, doi: 10.1109/SmartIoT52359.2021.00048.
7. Sylvain Grangeon, Céline Roux, Catherine Lerouge, Patrick Chardon, Romain Beuzeval, Gilles Montavon, Francis Claret, Thomas Grangeon, Geochemical and mineralogical characterization of streams and wetlands downstream a former uranium mine (Rophin, France), Applied Geochemistry, Vol.150, 2023, 105586.
8. Jeanette Rosas-Moreno, Christopher Walker, Katie Duffy, Claudia Krüger, Manuela Krüger, Clare H. Robinson, Jon K. Pittman, Isolation and identification of arbuscular mycorrhizal fungi from an abandoned uranium mine and their role in soil-to-plant transfer of radionuclides and metals, Science of The Total Environment, Vol. 876, 2023, 162781
9. Esther Erdei, Chris Shuey, Curtis Miller, Joseph Hoover, Miranda Cajero, Johnnye Lewis, Metal mixture exposures and multiplexed autoantibody screening in Navajo communities exposed to uranium mine wastes, Journal of Translational Autoimmunity, Vol. 6, 2023, 100201.
10. Ljubica Zupunski, Renée Street, Evgenia Ostroumova, Frank Winde, Susanne Sachs, Gerhard Geipel, Vusumuzi Nkosi, Liacine Bouaoun, Tanya Haman, Joachim Schüz, Angela Mathee, Environmental exposure to uranium in a population living in close proximity to gold mine tailings in South Africa, Journal of Trace Elements in Medicine and Biology, Vol. 77, 2023, 127141.
11. Hui Zhang, Jie Gao, Yunlong Bai, Lei Zhou, Lechang Xu, Delimiting radiation protection distance of underground uranium mining and metallurgy facilities: A case study in China, Heliyon, Vol. 8, Issue 12, 2022, e12419.
12. Young-Yong Ji, Sungyeop Joung, Byung Il Min, Kyung-Suk Suh, Development of Airborne Gamma-Ray Spectrometer Based on a CZT detector, Transactions of the Korean Nuclear Society Virtual Autumn Meeting, December 17-18
13. C. Budtz-Jorgensen, I. Kuvvetli, Y. Skogseide, K. Ullaland and N. Ostgaard, "Characterization of CZT Detectors for the ASIM Mission," in IEEE Transactions on Nuclear Science, vol. 56, no. 4, pp. 1842-1847, Aug. 2009, doi: 10.1109/TNS.2009.202142